Dynamics of spiral waves under global feedback in excitable domains of different shapes

Vladimir Zykov and Harald Engel
Institut für Theoretische Physik, Technische Universität Berlin, Hardenbergstrasse 36, D-10623 Berlin, Germany
(Received 1 October 2003; revised manuscript received 4 March 2004; published 8 July 2004)

It is found that the dynamics of spiral waves subjected to global feedback is extremely sensitive to the domain shape. Bifurcations in the velocity field which specifies the resonant drift of the spiral wave core induced by global feedback are analyzed. It is shown, for example, that smooth variation of the eccentricity of an elliptical domain induces a cascade of bifurcations that can dramatically change the spiral wave evolution. In a square domain a set of point attractors appears instead of the circular resonance attractor typical of a circular domain. These predictions are in good quantitative agreement with numerical integrations of an excitable reaction-diffusion system performed under global feedback.

DOI: 10.1103/PhysRevE.70.016201 PACS number(s): 05.45.−a, 05.65.+b, 47.54.+r, 82.40.Bj

I. INTRODUCTION

Pattern formation in distributed reaction-diffusion systems with nonlinear local kinetics is studied for application to quite different physical, biological and chemical media [1,2]. It has become clear in recent years that pattern evolution in many experimental systems is affected by some nonlocal effects, e.g., global feedback, when the local kinetics is influenced by the integral of the activity taken over the whole medium in a confined geometry. Examples of experimental systems that include such global feedback are an electrically heated catalytic surface, the average temperature of which is kept constant [3], ac gas discharge between two glass plates [4], a catalytic surface kept in a continuously stirred tank reactor (CSTR) [5], semiconductor devices [6], etc.

Recent experimental investigations of the Belousov–Zhabotinsky (BZ) reaction [7,8] and catalytic CO oxidation on platinum [9] proved that global feedback can be used efficiently to control pattern formation processes. Theoretical study demonstrates that global feedback creates conditions for the appearance of quite new or the stabilization of known spatio-temporal patterns [10–13].

A spiral wave (a pattern typical in excitable media) can be also effectively manipulated using global feedback as was found in numerical computations [14] and in experiments with the BZ reaction [15]. Such control is important for different applications, e.g., low voltage defibrillation of cardiac tissue [16,17].

It was shown recently that the size of the excitable domain is a very important control parameter, in addition to other very common ones like the time delay and gain in the feedback loop [18,19]. For instance, the stability conditions of a rigidly rotating spiral placed near the center of a circular domain directly depend on the domain size. Moreover, on disks of sufficiently large size, global feedback induces motion of the spiral wave core along a closed circular orbit (the so-called resonance attractor) [15,19,20].

Up to now the role of domain shape has not been studied systematically in relation to reaction-diffusion systems with global feedback. Circular- or square-shaped domains are commonly used in experiments and computations as they are the two simplest types of two-dimensional confined geometry [7,9,11,14,16]. The only well established result is that in two-dimensional domains the variety of spatio-temporal patterns is much broader than in one-dimensional systems [11].

Numerical and experimental results reported recently [20] demonstrate a strong difference in spiral wave dynamics in circular and elliptical domains subjected to global feedback. In this work the influence of domain shape on the evolution of spiral waves is investigated in more detail. The basic idea is to determine a velocity field that specifies the resonant drift induced by global feedback in domains of different shape. The study is based on a generic description of excitable media using only minimal information about their properties. The main assumption is that the feedback signal is so small that the drift induced is slow. The results of this simplified consideration are compared with numerical data obtained by integration of a specific reaction-diffusion model.

II. MATHEMATICAL MODEL

It is well known that the qualitative dynamic features of wave processes in reaction-diffusion systems are rather robust and insensitive to the exact form of mathematical model applied [1,2,21]. We use below a two-component model,

$$\frac{\partial u}{\partial t} = D_u \nabla^2 u + F(u,v) - I(t),$$

$$\frac{\partial v}{\partial t} = \epsilon G(u,v), \tag{1}$$

where variables $u(x,y,t)$ and $v(x,y,t)$ can be interpreted as concentrations of the reagents within a thin (quasitwo-dimensional) reaction layer. The function $I(t)$ specifies the external forcing (e.g., illumination of the light-sensitive BZ solution) applied uniformly to the whole simulated domain.

For the functions $F(u,v)$ and $G(u,v)$ we take the form used earlier in Refs. [14,19–21]:

$$F(u,v) = f(u) - v,$$

$$f(u) = \begin{cases} -k_1 u, & u \leqslant \sigma, \\ k_f(u-a), & \sigma < u < 1-\sigma, \\ k_2(1-u), & 1-\sigma \leqslant u, \end{cases}$$

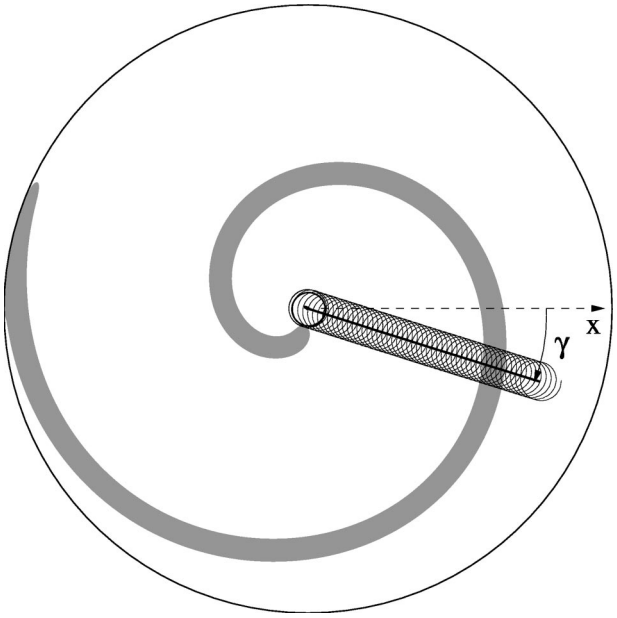

FIG. 1. Resonant drift of a spiral wave in a circular domain with radius $R_d=3\lambda$ induced by periodic forcing $I(t)=0.02\cos(\omega t)$. The excitable medium is described by system (1) and (2). In the shaded region $v(x,y,0)\geqslant 0.2$. The trajectories of the spiral wave tip (thin solid curve) and of the spiral core (thick solid line) are shown. The direction of drift is specified by the angle $\gamma\approx -0.1\pi$.

$$G(u,v)=\begin{cases} k_g u - v, & k_g u - v \geqslant 0, \\ k_\epsilon (k_g u - v), & k_g u - v < 0, \end{cases} \tag{2}$$

with the following parameter values: $k_f=1.7$, $k_g=2$, $k_\epsilon=6.0$, $a=0.1$, $\sigma=0.01$, $\epsilon=0.3$, and $D_u=1$. Parameters k_1 and k_2 are chosen in such a way that function $f(u)$ is continuous at $u=\sigma$ and $1-\sigma$.

This system has a single uniform rest state $[u(x,y)=v(x,y)=0]$ which is stable with respect to small perturbations. However, suprathreshold perturbation applied to the rest state or specific initial conditions can lead to undamped propagation of excitation waves. Both these properties are common features of a generic excitable medium.

System (1), (2) was integrated for domains of different shape with time step $\Delta t=0.02$, and space step $h=0.4$ under Dirichlet conditions at boundary Γ $(u|_\Gamma=0)$ corresponding to the common experimental situation where a piece of gel with an immobilized catalyst is placed into BZ solution.

In the autonomous system (1) and (2) with $I(t)=0$, by choosing appropriate initial conditions, a rigidly rotating spiral wave can be created in a circular domain as illustrated in Fig. 1. The measured period of this rotation is $T=2\pi/\omega=51.38$ and the spiral pitch is $\lambda=64.0$.

III. RESONANT DRIFT OF SPIRAL WAVES

Without external forcing [i.e., when $I(t)=0$] the spiral wave tip [the point where $u(x,y,t)=0.6$ and $\partial u/\partial t=0$] describes a circular orbit of radius $R_q=5.87=0.092\lambda$. Small periodic variations of $I(t)$ induce deformation of the tip trajectory and lead to resonant drift of the spiral wave core as shown in Fig. 1. Theoretical [22–25] and experimental [26–28] investigations suggest that the resonant drift is a general property of excitable media regardless of their local kinetics.

The direction of the drift, of course, depends on the initial orientation of the spiral, which will be specified below by the angle Θ_0. This value represents the initial orientation of an Archimedean spiral that approximates a spiral wave front far away from the core center:

$$\Theta(r,t)=\Theta_0-\frac{2\pi}{\lambda}r+\omega t, \tag{3}$$

where (Θ,r) are polar coordinates with their origin at the core center. For example, the front of the spiral shown in Fig. 1 is approximated at $t=0$ by an Archimedean spiral (3) with $\Theta_0=0$, since at the intersection with the boundary we have $\Theta(3\lambda/2,0)=-3\pi$.

Assume that for $\Theta_0=0$ weak resonant modulation $I(t)=A\cos(\omega t)$ induces drift specified by angle $\gamma=\varphi$ (see Fig. 1). Angle φ is a characteristic of the given medium. If the spiral is initially turned by angle $\Theta_0\neq 0$, the drift direction will also be turned by Θ_0, i.e., $\gamma=\varphi+\Theta_0$. On the other hand, modulation in the form of $I(t)=A\cos(\omega t-\phi_m)$ with phase ϕ_m can be considered as modulation with $\phi_m=0$, but with the initial spiral orientation taken at time $t_0=\phi_m/\omega$. Thus, for arbitrarily chosen Θ_0 and ϕ_m the drift direction can be written as

$$\gamma=\varphi+\Theta_0+\omega t_0=\varphi+\Theta_0+\phi_m. \tag{4}$$

The parameter φ can be determined analytically if the underlying model of the excitable medium satisfies some special conditions [22,25]. However, for an arbitrary form of functions $F(u,v)$ and $G(u,v)$ in system (1) this problem is unsolved. In our case, Eqs. (2), this constant has been determined numerically by computations of resonant drift with well defined values of Θ_0 and ϕ_m. The resonant drift computed for $\Theta_0=0$ and $\phi_m=0$ is illustrated in Fig. 1. The value of drift angle obtained is $\gamma=-0.1\pi$. Substituting these values into Eq. (4) we get $\varphi=-0.1\pi$. This value will be used below where the direction of drift induced by global feedback is determined.

IV. DRIFT VELOCITY INDUCED BY GLOBAL FEEDBACK

To realize global feedback the modulation signal $I(t)$ is computed as [14,20]

$$I(t)=k_{fb}(B(t-\tau)-B_0), \tag{5}$$

where

$$B(t)=\frac{1}{S}\int_S v(x',y',t)dx'dy'. \tag{6}$$

Thus, the feedback signal is proportional to the integral value B of the second variable over the simulated domain of area S taken with time delay τ. Constant B_0 in Eq. (5) is the value of

this integral for a spiral wave that is rigidly rotating exactly around the center of a circular domain (for the model used $B_0=0.1$). The gain k_{fb} is fixed in the computations performed below at $k_{fb}=0.1$.

If the spiral wave core is displaced with respect to the center of the circular domain, the computed integral $B(t)$ and, hence, the modulation signal $I(t)$ should be periodic functions of time with period T. It is known that only the first component in the Fourier series of a weak periodic modulation induces resonant drift [22,24]. A general expression for this first component is

$$I(t) = k_{fb}A(x,y)\cos[\omega t - \omega\tau + \Theta_0 - \phi(x,y)], \tag{7}$$

where (x,y) are the coordinates of the center of the spiral wave core, and $A(x,y)$ and $\phi(x,y)$ are the amplitude and the phase of the first Fourier component of $B(t)$. The amplitude $A(x,y)$ determines the absolute value of the drift velocity and the drift direction depends on the phase $\phi_m(x,y)=\omega\tau-\Theta_0+\phi(x,y)$ [22–25]. It follows from Eqs. (4) and (7) that the direction of drift induced by global feedback can be expressed as

$$\gamma(x,y) = \varphi + \omega\tau + \phi(x,y). \tag{8}$$

In contrast to Eq. (4) the drift direction determined by Eq. (8) does not depend on the initial orientation of the spiral specified by Θ_0. Thus, if the drift induced is so slow that the shape and the angular velocity of the rotating spiral always remain the same, motion of the core center induced by feedback can be described by a system of two ordinary differential equations [20]:

$$\frac{dx}{dt} = V(A)\cos\ \gamma, \tag{9}$$

$$\frac{dy}{dt} = V(A)\sin\ \gamma, \tag{10}$$

where V is the absolute value of the drift velocity [$V(A)\sim k_{fb}A(x,y)$ for slow drift] and $\gamma=\gamma(x,y)$ is specified by Eq. (8).

In weakly excitable media a spiral wave has the form of a thin curved stripe (see Fig. 1). In this case the integral B should be proportional to the arc length L of the spiral wave front: $B=\beta L/S$, where β is a positive constant. By approximating the shape of the front by an Archimedean spiral [21,29,30], the determination of the amplitude $A(x,y)$ and the phase $\phi(x,y)$ can be reduced to a purely geometrical procedure. Imagine that the center of an Archimedean spiral described by Eq. (3) with $\Theta_0=0$ is placed at a point (x,y). Then the arc length L of the spiral within a domain of given shape should be a periodic function of time and the first Fourier component of this function gives us the amplitude $A(x,y)$ and the phase $\phi(x,y)$, which determines the direction of drift in accordance with Eq. (8).

The velocity field obtained by application of the procedure described for a circular domain of radius $R_d=1.5\lambda$ is shown in Fig. 2. The drift velocity [which is proportional to amplitude $A(x,y)$] vanishes at the domain center and represents an unstable node. This unstable node is surrounded by a closed circular orbit of radius about 0.62λ. At all points of this orbit the drift velocity is orthogonal to the radial direction, i.e., it is oriented exactly tangential to the orbit. In the vicinity of this orbit the radial component of the drift velocity is positive at points located closer to the domain center and negative at the opposite side. Hence, this closed orbit is a stable limit cycle. Due to the rotational symmetry of the domain, the amplitude $A(x,y)$ and, hence, the absolute value of the drift velocity $V(x,y)$ are constant on the limit cycle. The drift direction along this orbit coincides with the rotational direction of the spiral wave that is counterclockwise in the case considered.

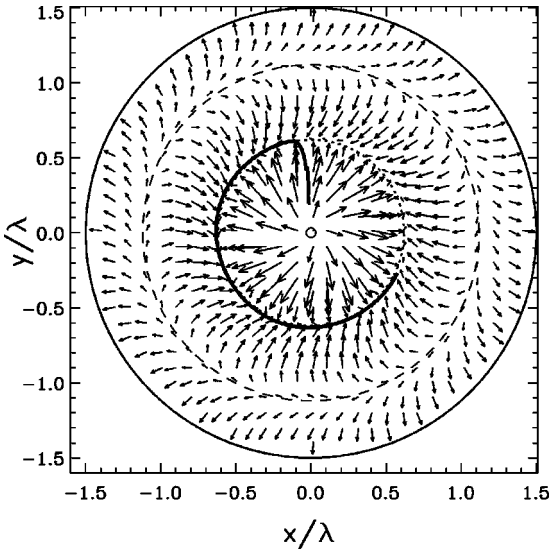

FIG. 2. Drift velocity field of the spiral core induced by global feedback according to Eq. (5) ($\tau=0$) in a circular domain of radius $R=3\lambda$. Calculations of the velocity field are based on the Archimedean spiral approximation. The open circle indicates an unstable fixed point at the domain center. The dotted (dashed) circle shows the stable (unstable) limit cycle. The trajectory of the core center computed from reaction-diffusion model (1) and (2) is shown by the thick solid curve.

There is another circular orbit of radius about $1.12\ \lambda$ where the radial component of the drift velocity vanishes. Here the tangential component is directed clockwise. This closed trajectory is unstable, since the radial component in its vicinity is oriented away from it (see Fig. 2).

The stable limit cycle is the resonance attractor of spiral waves [19]. If the center of a spiral wave is initially located somewhere between the domain center and the unstable cycle due to feedback-induced resonant drift it will approach the stable limit cycle. The trajectory of the core center computed from reaction-diffusion system (1) and (2) (thick solid curve in Fig. 2) agrees very well with the velocity field obtained.

V. DRIFT VELOCITY FIELD IN AN ELLIPTICAL DOMAIN

Figure 3 shows the velocity field that corresponds to an excitable domain of elliptical shape. The large axis of the

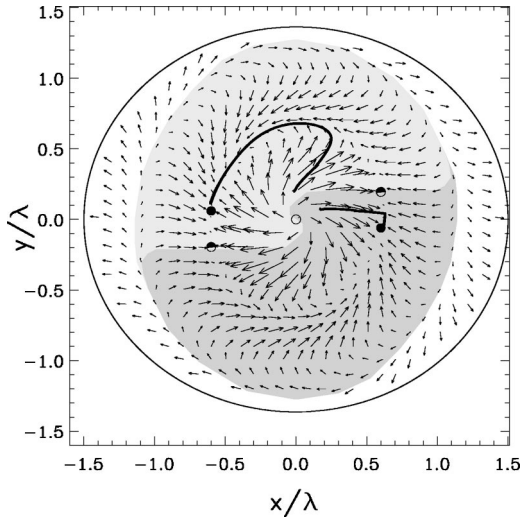

FIG. 3. Drift velocity field of the spiral core induced by global feedback according to Eq. (5) ($\tau=0$) in an elliptical domain with $a/b=1.1$. Calculations of the velocity field are based on the Archimedean spiral approximation. Half-closed circles denote saddles. Closed (open) circles indicate stable (unstable) nodes. The basins of attraction of stable fixed points are shown by different gray levels. The trajectories of the core center computed from reaction-diffusion model (1), (2) for two different initial locations of the spiral wave are shown by thick solid curves.

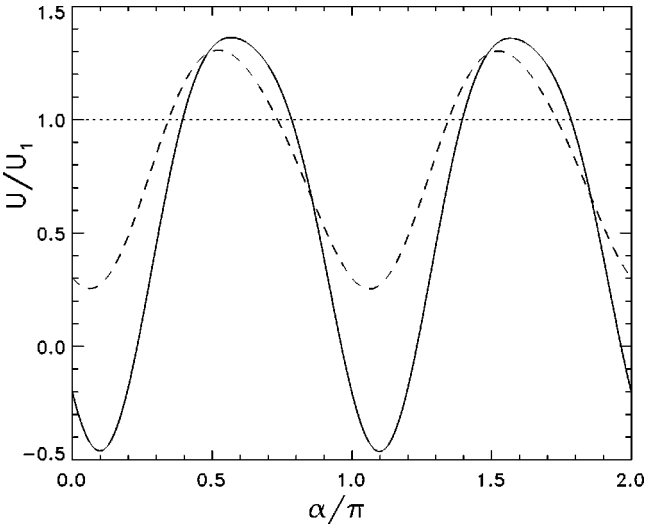

FIG. 4. Tangential component of the drift velocity along the circular orbit shown in Fig. 2 computed for two elliptical domains with different eccentricity. Solid and dashed curves were computed for $a/b=1.1$ and 1.05, respectively. The dotted line represents computations for a circular domain.

ellipse$a$ is equal to 3λ and its ratio to small axis b is equal to $a/b=1.1$. Even this small deviation from circular shape dramatically changes the velocity field plotted in Fig. 2. The limit cycle corresponding to the resonance attractor is destroyed and two pairs of new fixed points appear where the drift velocity vanishes. One fixed point in each pair is a saddle and the other one is a stable node. Depending on the initial conditions, the spiral wave will approach one of the two stable nodes. The velocity field computed allows one to sketch corresponding basins of attraction. Trajectories of the core center obtained by numerical integration of Eqs. (1) and (2) for two different initial locations of the core are shown by thick solid curves in Fig. 3. These computations are in perfect agreement with the velocity field predicted by applying the Archimedean spiral approximation.

The observed bifurcation can be studied in more detail by considering the drift velocity computed for points at the limit cycle in the circular domain (see Fig. 2). To this end it is convenient to specify the location of points along this limit cycle by a polar angle α counted from the X axis. For each of these points a value of $U(\alpha)$ can be found that is the projection of the drift velocity on the tangent to the limit cycle. Figure 4 shows $U(\alpha)$ computed for two elliptical domains with different values of the ratio a/b. The case of $a/b=1$ corresponds to the circular domain, where the velocity along the limit cycle remains constant, $U(\alpha)=U_1>0$ (dotted line in Fig. 4).

Small deformation of the circular shape breaks down the rotational symmetry of the domain and the drift velocity on the limit cycle is no longer constant. Instead, as a function of α it starts to oscillate around U_1. For small eccentricity ($a/b=1.05$) the amplitude of these oscillations remains relatively small (dashed curve in Fig. 4) and exerts only a quantitative influence on the spiral wave dynamics. The former limit cycle in a circular domain is not yet destroyed and qualitatively the dynamics of the drift induced remains the same.

For the elliptical domain shown in Fig. 3 ($a/b=1.1$) the corresponding velocity along the former limit cycle is shown in Fig. 4 by the solid curve. In this case $U(\alpha)$ so strongly deviates from U_1 that it even becomes negative at some segments of the circular orbit. Four values of α at which $U(\alpha)=0$ correspond to the four fixed points that appeared due to bifurcation shown in Fig. 3. Since beyond bifurcation the points at the former limit cycle remain attracting in the radial direction (compare the orientation of the radial component of the drift induced near the orbit in Fig. 3), two of these fixed points are classified as stable nodes, the two others as saddles.

The saddle-node bifurcation responsible for the qualitative change in spiral dynamics occurs at $a/b\approx 1.07$. At this value deformation of the circular domain becomes so large that the drift velocity vanishes at two points of the former limit cycle. These points are located diametrically opposite on a line which is turned in the counterclockwise direction with respect to the X axis.

Further increase of the ratio a/b induces additional bifurcations. For instance, at $a/b=1.3$ the velocity field has already nine fixed points (see Fig. 5). Two additional saddle-node pairs appear due to a second bifurcation that occurs at $a/b\approx 1.2$. In comparing Figs. 3 and 5 one finds that the "old" saddle-node pairs that appeared due to the first bifurcation do not undergo any qualitative changes. Nodes in these pairs remain stable and their locations are practically the same. The only difference induced by additional deformation of the domain is an increase in distance between the node and saddle in both pairs.

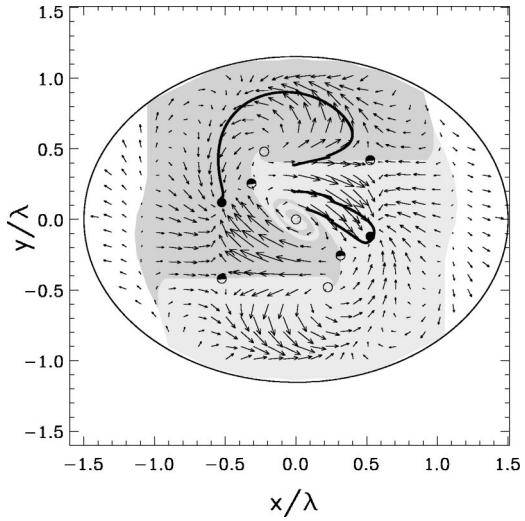

FIG. 5. Drift velocity field of the spiral core induced by global feedback according to Eq. (5) ($\tau=0$) in an elliptical domain with $a/b=1.3$. Calculations of the velocity field are based on the Archimedean spiral approximation. Half-closed circles denote saddles. Closed (open) circles indicate stable (unstable) fixed points. The basins of attraction of stable fixed points are shown by different gray levels. The trajectories of the core center computed from reaction-diffusion model (1) and (2) for three different initial locations of the spiral wave are shown by thick solid curves.

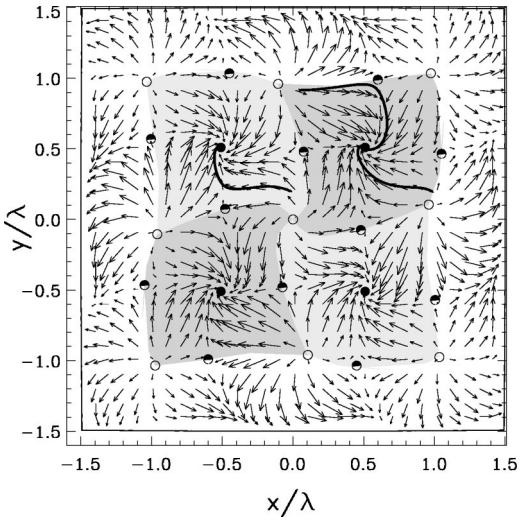

FIG. 6. Drift velocity field of the spiral core induced by global feedback according to Eq. (5) ($\tau=0$) in a square-shaped domain of size 3λ. Calculations of the velocity field are based on the Archimedean spiral approximation. Closed (open) circles indicate stable (unstable) nodes. Half-closed circles denote saddles. The basins of attraction of stable fixed points are shown by different gray levels. The trajectories of the core center computed from reaction-diffusion model (1) and (2) for three different initial locations of the spiral wave are shown by thick solid curves.

In the last saddle-node pairs created the nodes are unstable. Hence, no additional attracting points appear in the domain. However, the trajectories of the induced drift look quite different in comparison to those observed for $a/b=1.1$. Two of the core center trajectories shown in Fig. 5 are computed starting from the same initial conditions as those shown in Fig. 3. However, now both trajectories approach the same stable node, while in Fig. 3 they were going toward two different ones. In order to reach the left stable node the initial location should be shifted far away from the domain center (see the third trajectory in Fig. 5). Hence, the dynamics of spiral drift becomes more sensitive to the initial location if the domain deformation increases.

VI. VELOCITY FIELD IN A SQUARE-SHAPED DOMAIN

The velocity field related to a square-shaped domain of size 3λ (seen in Fig. 6) is much more complicated than that computed for a circular domain. It contains 13 nodes and 12 saddles. One node, located exactly at the domain center, is unstable as is the center node in the circular domain of diameter 3λ (see Fig. 2). Four nodes located at the corners of a square of size about λ are stable and play the role of attractors of drifting spiral waves. The velocity field obtained in the Archimedean spiral approximation allows one to predict what kind of stable nodes will be reached starting from a given initial spiral wave location. Trajectories of the core center computed from the reaction-diffusion model (1) and (2) coincide well with these predictions (thick solid curves in Fig. 6).

Eight other nodes located approximately at the corners and sides of a square of size 2λ are unstable. The saddles are also arranged rather regularly. The locations of all fixed points are invariant under rotation of the domain by an angle of $\pi/2$.

Obviously, the jump from a circular- to a square-shaped domain induces strong disturbances in the spiral wave dynamics. In order to clarify bifurcations that result in the appearance of this complicated velocity field continuous deformation of the domain shape should be applied.

To do this a specially shaped excitable domain is used which is bounded by four arcs of radius $R_b \geqslant R_d$ as shown in Fig. 7. The left arc is centered at point $(R_b-R_d,0)$ marked by a cross in Fig. 7(a). Hence, this arc touches the left side of the square at point $(-R_d,0)$ and this side of the square is tangent to the arc. Similar rules specify the location of the other three arcs. Obviously, if $R_b=\infty$ the domain shape is square, while for $R_b=R_d$ it has a circular shape. Thus, smooth transformation from a circular- to a square-shaped domain can be performed if ratio R_d/R_b is continuously decreased from $R_d/R_b=1$ to 0.

Figure 7(a) shows the computed velocity field that corresponds to the relatively small deformation ($R_d/R_b=0.65$) of the circular domain with radius $R_d=1.5\lambda$. Four saddle-node pairs appear and destroy the limit cycle in the circular domain (cf. Fig. 2). A corresponding saddle-node bifurcation takes place at $R_d/R_b\approx 0.7$. Further decrease of the ratio R_d/R_b causes a second bifurcation at $R_d/R_b\approx 0.6$. The velocity field computed near this bifurcation at $R_d/R_b=0.5$ is shown in Fig. 7(b), where four new saddle-node pairs have appeared. The newly created nodes are unstable in contrast to those that appear due to the first bifurcation.

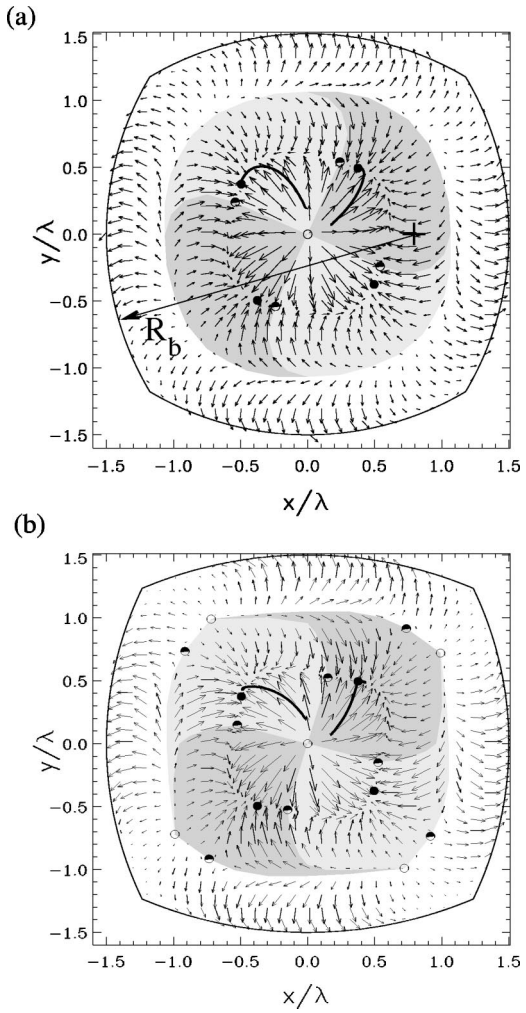

FIG. 7. Drift velocity field of the spiral core induced by global feedback according to Eq. (5) ($\tau=0$) in two arc-bounded domains. $R_d/R_b=$(a) 0.65 and (b) 0.5. Calculations of the velocity field are based on the Archimedean spiral approximation. Half-closed circles denote saddles. Open (closed) circles indicate unstable (stable) nodes. The basins of attraction of stable fixed points are shown by different gray levels. The trajectories of the core center computed from reaction-diffusion model (1) and (2) for two different initial locations of the spiral wave are shown by thick solid curves.

A third bifurcation occurs at $R_d/R_b\approx 0.3$ and results in the formation of four additional saddle-node pairs with unstable nodes. The velocity field computed at $R_d/R_b=0.2$ (not shown here) looks very similar to the limiting case of $R_d/R_b=0$ that corresponds to the square-shaped domain shown in Fig. 6.

As in the case of an elliptical domain, a saddle-node pair once created does not undergo any qualitative changes. However, the distance between the saddle and the node is continuously increased when the bifurcation parameter R_d/R_b becomes smaller.

VII. ROLE OF TIME DELAY

In all examples considered before, the time delay in the feedback loop was fixed to $\tau=0$ to focus on the role of domain shape, and that is the main purpose of this work. However, in order to complete the picture, in the following the influence of the time delay should be investigated.

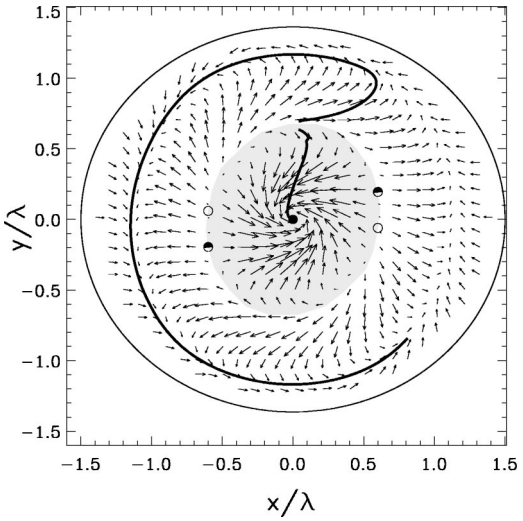

FIG. 8. Drift velocity field of the spiral core induced by global feedback according to Eq. (5) ($\tau=26$) in an elliptical domain with $a/b=1.1$. Calculations of the velocity field are based on the Archimedean spiral approximation. Half-closed circles denote saddles. Open (closed) circles indicate unstable (stable) nodes. The basins of attraction of stable fixed points are shown by different gray levels. The trajectories of the core center computed from reaction-diffusion model (1) and (2) for two different initial locations of the spiral wave are shown by thick solid curves.

First we note that the amplitude $A(x,y)$ computed in Eq. (7) does not depend on time delay τ. Only the direction of the drift determined by Eq. (8) depends on τ. Thus, the effect of the time delay consists of simultaneous rotation of all vectors in the drift velocity field by the same angle $\omega\tau$. Due to this, the phase field $\phi(x,y)$ computed for $\tau=0$ can be easily used to determine the velocity field for an arbitrary value of τ.

For example, if the time delay is about one half the rotation period T, the corresponding velocity field is the same as that obtained for $\tau=0$, except that the directions of all vectors are changed to opposite ones. In particular, stable nodes or limit cycles become unstable and vice versa.

To illustrate this important feature the velocity field for the elliptical domain with $a/b=1.1$ and $\tau=26\approx T/2$ is presented in Fig. 8. A comparison between Figs. 3 and 8 shows that the number and location of all fixed points remain the same. In fact, a fixed point appears at those sites (x,y), where the amplitude $A(x,y)$ vanishes. Since this function does not depend on the time delay, the locations of fixed points also do not depend on τ. However, both nodes, which were stable at $\tau=0$, become unstable at $\tau=T/2$ and the unstable node at the domain center transforms into a stable one (cf. Figs. 3 and 8). The stable and the unstable directions corresponding to a saddle at $\tau=0$ are changed to opposite ones if $\tau=T/2$ is applied.

The unstable closed orbit, which can be seen in Fig. 2 for $\tau=0$, is transformed into a stable limit cycle at $\tau=T/2$, which

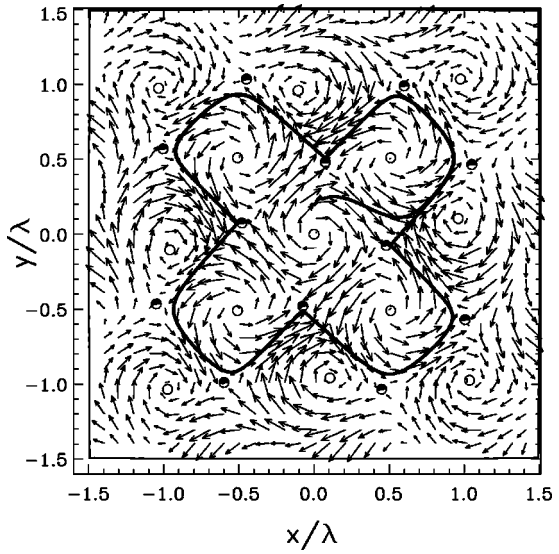

FIG. 9. Drift velocity field of the spiral core induced by global feedback according to Eq. (5) ($\tau=33$) in a square-shaped domain of size 3λ. Calculations of the velocity field are based on the Archimedean spiral approximation. Open circles indicate unstable nodes. Half-closed circles denote saddles. The trajectory of the core center computed from reaction-diffusion model (1) and (2) is shown by a thick solid curve.

represents now the resonance attractor of spiral waves. The center of a spiral core initially located somewhere outside the former stable orbit corresponding to $\tau=0$ approaches this stable limit cycle. If an initial location is chosen somewhere inside the former stable orbit, the spiral wave core approaches the domain center, where now a stable node is located. The corresponding trajectories computed for the reaction-diffusion model (1) and (2) are shown by thick solid lines in Fig. 8.

Hence, by initially choosing $\tau=T/2$, the bifurcation scenario induced by smooth variation of the eccentricity of an elliptical domain should look quite different compared to the case of $\tau=0$ considered above. For instance, the first saddle-node bifurcation at $a/b\approx1.07$ does not change the spiral wave dynamics as dramatically as at $\tau=0$. Figure 8 shows that two saddle-node pairs appear after this bifurcation, but they contain no attracting points. In contrast to this, a qualitative change of the velocity field should be expected after the second bifurcation at $a/b\approx1.2$, due to the formation of two stable nodes.

Another interesting example for the important role of the time delay was found in application to a square-shaped domain shown in Fig. 6. It is clear, that if $\tau=T/2$ all stable nodes in the drift velocity field become unstable and vice versa. However, in a narrow range of time delay near $\tau=0.65T$ all nodes shown in Fig. 6 become unstable. This unusual situation is illustrated by Fig. 9. In this case the trajectory of the core center starting near the domain center asymptotically achieves a stable close orbit that represents the resonance attractor of spiral waves. Its shape considerably differs from the circular orbit observed in a circular domain.

Thus, the impact of the shape of a confined domain on the spiral wave dynamics strongly depends on the other parameters of the excitable system under consideration, particularly on the time delay in the global feedback loop.

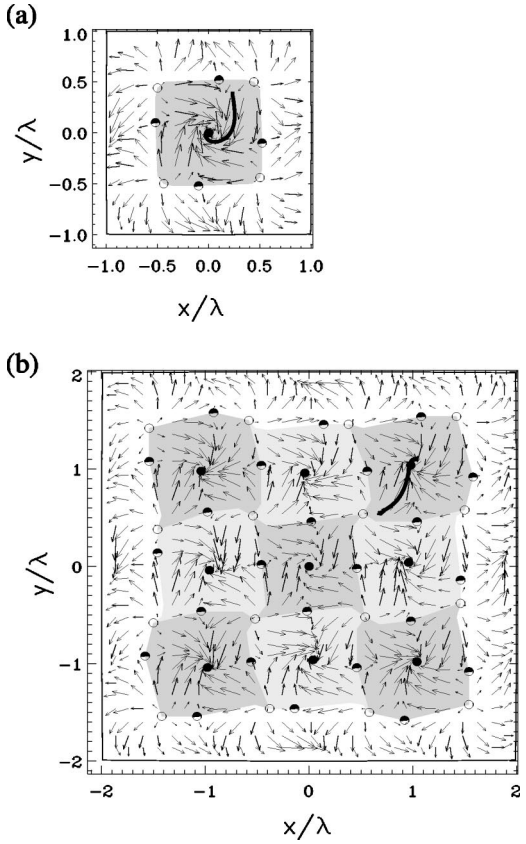

FIG. 10. Drift velocity field of the spiral core induced by global feedback according to Eq. (5) ($\tau=0$) in a square-shaped domain of size 2λ (a) and 4λ (b). Calculations of the velocity field are based on the Archimedean spiral approximation. Half-closed circles denote saddles. Closed (open) circles indicate stable (unstable) nodes. The basins of attraction of stable fixed points are shown by different gray levels. The trajectories of the core center computed from reaction-diffusion model (1) and (2) are shown by thick solid curves.

VIII. ROLE OF DOMAIN SIZE

Figure 10 illustrates the impact of the domain size on the spiral wave dynamics induced by global feedback. The first conclusion following from a comparison between Figs. 10(a) and 10(b) is that the complexity of the drift velocity fields dramatically increases with the domain size. On the other hand, one can find regularity in this increase of complexity. The drift velocity field computed for the squared-shaped domain of size 2λ contains only one stable node. The basin of attraction of this node is restricted by separatrixes of four saddles beginning at four unstable nodes. It is important to stress that topologically similar cells that contain one center node surrounded by four saddles and four nodes also can be found in square-shaped domains of larger sizes [see Figs. 6 and 10(b)]. The exact shape of these cells is slightly different, but they all have the same characteristic size of about λ

and are adjoined side to side. While in the square domain of size 2λ there is room for only one such cell, domains of 3λ and 4λ already include four and nine cells, respectively. Thus, in a square-shaped domain of size $n\lambda$ the number of elementary cells is expected to be $(n-1)^2$.

The cellular structure of the drift velocity field is a characteristic feature of a square-shaped domain in contrast to a circular domain, where closed circular orbits constitute a family of limit cycles, rather than a set of fixed points [19]. In a disk of sufficiently large size, stable limit cycles (resonance attractors) are located concentrically with spacing λ. Unstable limit cycles separate neighboring basins of attraction and are also located concentrically with spatial period λ [19]. Thus, the main conclusion that the complexity of the drift velocity field increases with the domain size and some periodicity of basins of attraction takes place represents a rather general rule.

Another important conclusion can be made about the stability of the fixed point at the middle of the square. This fixed point is stable if the domain size is $n=2$ or 4 and unstable when $n=3$. Thus, with a monotonous increase of the domain size the stability and instability of the middle point alternate periodically. Similar periodicity has been observed in the case of a circular domain [18,19]. Moreover, the stability of the center point in a circular domain has been studied analytically [19]. Using these results it is easy to see that phase $\phi(x,0)$ of the feedback signal for small displacement $x \ll \lambda$ of the core center with respect to the domain center obeys the following expression:

$$\phi(x,0) = \pi(n-1), \tag{11}$$

where n is the diameter of the circular domain expressed in units of λ. Thus, an increase of the domain size from n to $n+1$ results in a quite opposite drift direction, and a stable (unstable) center point becomes unstable (stable). The same rule is obviously valid for the stability of the middle point in a square-shaped domain with diameter n of an inscribed circle.

It is important also to mention that the critical eccentricity of an elliptical domain corresponding to the observed saddle-node bifurcations depends on the domain size. For instance, in this work an elliptical domain with large axis of $a=3\lambda$ is analyzed and the first bifurcation occurs at $a/b \approx 1.07$. If the large axis $a=2\lambda$ the bifurcation takes place at $a/b \approx 1.2$ [20].

IX. DISCUSSION

The study performed demonstrates the diversity of spiral waves dynamics in excitable domains of different shapes subjected to global feedback. As an extension of the recently reported experimental and computational results related to spiral wave drift in elliptical domains [20] a much more systematic study was performed. It was shown that under smooth variation of the eccentricity of an elliptical domain even relatively small deformation of the domain shape can result in a dramatic change in the spiral wave dynamics due to saddle-node bifurcation in the velocity field of the resonant drift (cf. Figs. 2 and 3). It was found that further increase of the eccentricity results in a second bifurcation in the drift velocity field (Fig. 5). In addition to elliptical domains of different eccentricity, square-shaped domains of different sizes (cf. Figs. 6 and 10) and a smooth transition from a circular domain to a square-shaped one were considered (Fig. 7).

A comparison of Figs. 2 and 6 demonstrates how dramatic the influence of the domain shape on the spiral wave dynamics can be. This has to be kept in mind when a square-shaped excitable domain is used in experiments with a reaction-diffusion system under global feedback.

For symmetry reasons it is clear that in an elliptical domain the simultaneous appearance of two saddle-node pairs is expected. It was demonstrated that a circular domain can be smoothly transformed into a square-shaped one and conserve invariance with respect to the rotation by $\pi/2$ (see Fig. 7). The complicated velocity field shown in Fig. 6 is the result of three successive saddle-node bifurcations, each of which led to the simultaneous appearance of four saddle-node pairs.

Up to now there has been no analytical way to describe the observed saddle-node bifurcations which are responsible for the appearance of new fixed points due to smooth deformation of a given domain. However, the proposed approach based on the Archimedean spiral approximation considerably simplifies the underlying description in terms of a nonlinear reaction-diffusion model subjected to global feedback. Due to this simplification analytical study of the problem is an interesting challenge for future work.

Our study demonstrated that the method for determination of the drift velocity field proposed recently [20] can be effectively applied to domains of different size and shape. However, to provide a quantitatively correct velocity field the distance from the spiral core center to the boundary should be large enough (at least more than two R_q), otherwise the boundary influence becomes essential. Due to these boundary effects the radius of the resonance attractor can differ from that in theoretical predictions [19]. Moreover, boundary effects can induce spiral drift along a Neumann boundary even without global feedback [14,31,32].

If the domain size is larger than the spiral wave pitch λ, the spiral wave dynamics becomes more diverse since the drift velocity field can contain multiple attractors. Boundary conditions (Dirichlet or Neumann type) have practically no influence on the spiral wave drift induced by global feedback in a domain of such size, and the method applied is especially precise. On the other hand, if the domain size exceeds about 10λ, the feedback mechanism ceases to be effective since alternations the feedback signal becomes very weak and comparable with the level of noise.

Note that in all the cases considered induced drift of a counterclockwise rotating spiral was investigated. Velocity fields in the case of a clockwise rotating spiral can be obtained as a mirror image of the ones presented.

In summary, the shape of the excitable domain proved to be a very essential control parameter for spiral wave dynamics under global feedback. This paper focused on the role of the domain shape keeping other control parameters (the size of the domain, the time delay τ and the gain k_{fb}) constant. Very preliminary considerations of the role of the time delay and the domain size show that they can essentially change

the dynamical behavior of spiral waves. A more detailed investigation of spiral wave dynamics under simultaneous variations of these control parameters is an interesting challenge for future theoretical and experimental study.

ACKNOWLEDGMENT

The authors thank the Deutsche Forschungsgemeinschaft (DFG Grant No. SFB 555) for financial support.

[1] *Wave and Patterns in Biological and Chemical Excitable Media*, edited by V. Krinsky and H. Swinney (North-Holland, Amsterdam, 1991).
[2] *Chemical Waves and Patterns*, edited by R. Kapral and K. Showalter (Kluwer, Dordrecht, 1995).
[3] Y. E. Volodin, V. V. Barelko, and A. G. Merzhanov, Sov. J. Chem. Phys. **5**, 1146 (1982).
[4] C. Radehaus, K. Kardell, H. Baumann, P. Jäger, and H.-G. Purwins, Z. Phys. B: Condens. Matter **65**, 515 (1987).
[5] S. L. Lane and D. Luss, Phys. Rev. Lett. **70**, 830 (1993).
[6] E. Schöll, *Nonlinear Spatio-temporal Dynamics and Chaos in Semiconductors* (Cambridge University Press, Cambridge, 2001).
[7] V. K. Vanag, L. Yang, M. Dolnik, A. M. Zhabotinsky, and I. Epstein, Nature (London) **406**, 389 (2000).
[8] E. Mihaliuk, T. Sakurai, F. Chirila, and K. Showalter, Phys. Rev. E **65**, 065602 (2002).
[9] M. Kim, M. Bertram, M. Pollman, A. von Oertzen, A. S. Mikhailov, H. H. Rotermund, and G. Ertl, Science **292**, 1351 (2001).
[10] K. Krischer and A. Mikhailov, Phys. Rev. Lett. **73**, 3165 (1994).
[11] U. Middya and D. Luss, J. Chem. Phys. **102**, 5029 (1995).
[12] M. Falcke, H. Engel, and M. Neufeld, Phys. Rev. E **52**, 763 (1995).
[13] H. Kori and Y. Kuramoto, Phys. Rev. E **63**, 046214 (2001).
[14] V. S. Zykov, A. S. Mikhailov, and S. C. Müller, Phys. Rev. Lett. **78**, 3398 (1997).
[15] O. Kheowan, C. K. Chan, V. S. Zykov, O. Rangsiman, and S. C. Müller, Phys. Rev. E **64**, 035201(R) (2001).
[16] A. V. Panfilov, S. C. Müller, V. S. Zykov, and J. P. Keener, Phys. Rev. E **61**, 4644 (2000).
[17] D. J. Christini and L. Glass, Chaos **12**, 732 (2002).
[18] O. Kheowan, V. S. Zykov, and S. C. Mueller, Phys. Chem. Chem. Phys. **4**, 1334 (2002).
[19] V. S. Zykov and H. Engel, Phys. Rev. E **66**, 016206 (2002).
[20] V. S. Zykov, G. Bordiougov, H. Brandtstädter, I. Gerdes, and H. Engel, Phys. Rev. Lett. **92**, 018304 (2004).
[21] V. S. Zykov, *Simulation of Wave Processes in Excitable Media* (Manchester University Press, Manchester, UK, 1987).
[22] V. A. Davydov, V. S. Zykov, and A. S. Mikhailov, Usp. Fiz. Nauk **161**, 45 (1991) [Sov. Phys. Usp. **34**, 665 (1991)].
[23] V. N. Biktashev and A. V. Holden, J. Theor. Biol. **169**, 101 (1994).
[24] R. M. Mantel and D. Barkley, Phys. Rev. E **54**, 4791 (1996).
[25] V. Hakim and A. Karma, Phys. Rev. E **60**, 5073 (1999).
[26] K. I. Agladze, V. A. Davydov, and A. S. Mikhailov, JETP Lett. **45**, 767 (1987).
[27] M. Braune, A. Schrader, and H. Engel, Chem. Phys. Lett. **222**, 358 (1994).
[28] S. Grill, V. S. Zykov, and S. C. Müller, J. Phys. Chem. **100**, 19082 (1996).
[29] N. Wiener and A. Rosenblueth, Arch. Inst. Cardiol. Mex **16**, 205 (1946).
[30] A. T. Winfree, Science **175**, 634 (1972).
[31] E. V. Nikolaev, V. V. Biktashev, and A. V. Holden, Chaos, Solitons Fractals **9**, 363 (1998).
[32] H. Brandstädter, M. Braune, I. Schebesch, and H. Engel, Chem. Phys. Lett. **323**, 145 (2000).